Early View publication on www.interscience.wiley.com
(issue and page numbers not yet assigned;
citable using Digital Object Identifier – **DOI**)

Phys. Status Solidi RRL, 1–3 (2010) / **DOI** 10.1002/pssr.201004258

pss +++rapid research letters+++
www.pss-rapid.com

# Frequency dependent power efficiency of a nanostructured surface plasmon coupler

**Amitabh Ghoshal and Pieter G. Kik***

CREOL, The College of Optics and Photonics, University of Central Florida, 4000 Central Florida Blvd, Orlando, FL 32816, USA

Received 8 June 2010, revised 7 July 2010, accepted 8 July 2010
Published online 13 July 2010

**Keywords** surface plasmons, plasmons, optical coupling, devices

* Corresponding author: e-mail kik@creol.ucf.edu, Phone: +31 407 823 4622, Fax: +31 407 823 6880

Surface plasmon (SP) excitation on an extended thin metal film via a miniature nanoparticle-enhanced grating coupler is studied experimentally using leakage radiation spectroscopy. A universally applicable method for determining the efficiency of free-space SP excitation is developed, and the efficiency of the coupler is determined. Two distinct grating excitation modes are observed, as well as a particle-mediated excitation mode. The maximum observed coupling efficiency of the structure was approximately 3.5% at 615 nm and 670 nm, corresponding to the two grating modes of the structure.



**1 Introduction** The field of integrated surface plasmon (SP) nanophotonics continues to develop rapidly due to the considerable advantages of SPs over traditional integrated photonic structures. The high degree of confinement of SPs at a single interface allows for various easily-fabricated single-interface waveguide designs [1–4]. Dielectric loaded SP waveguides [1] represent a promising approach, allowing for the development of SP based optical interconnects on standard silicon integrated circuits. To communicate with densely integrated plasmonic components, there is a need for a compact structure for coupling to SPs, and a corresponding need for a method for determining the coupling efficiency of any such structures.

Here we study a nanoparticle enhanced grating coupler for exciting SPs on a nearby metal film. We use a broadly applicable method to determine the absolute wavelength dependent coupling efficiency of the miniature coupler, and demonstrate the presence of both grating-mediated and particle resonance mediated SP excitation.

**2 Theory** We consider a 3-layer system extended infinitely in the $x,y$-plane consisting of a central metal layer of thickness $d$ surrounded by transparent semi-infinite cover and substrate layers. SPs are excited on the cover–metal interface via a nanostructured array illuminated from the top, and the refractive index of the substrate is chosen to be higher than that of the cover layer. Under these conditions, SPs at the top interface can generate leakage radiation (LR) in the substrate at a well-defined angle.

The SP excitation efficiency $\eta_{SP}$ by the array is defined as the ratio of the total power $P_{SP,tot}$ coupled into SPs propagating away from the array to the total power incident on the coupling structure $P_{inc}$. The total power deposited into propagating SPs is dissipated either radiatively or non-radiatively, giving $P_{SP,tot} = P_{SP,rad} + P_{SP,i}$ where $P_{SP,rad}$ is the power of the SP dissipated radiatively via LR into the substrate, and $P_{SP,i}$ is the power of the SP dissipated via intrinsic losses in the metal (non-radiative losses). In steady state, the power ratio of the radiative and intrinsic dissipation of the SP power is equal to the ratio of the dissipation rates: $P_{SP,i}/P_{SP,rad} = \Gamma_i/\Gamma_{rad}$. Here $\Gamma_{rad}$ is the radiative decay rate of the SP amplitude determined by the film thickness and the surrounding refractive indices, and $\Gamma_i$ is the intrinsic decay rate of the SP amplitude. Note that $\Gamma_i$ is related to but not equal to the electron scattering rate in the metal. Together, these considerations lead to the relation $\eta_{SP} = (P_{SP,rad}/P_{inc}) \times (1 + (\Gamma_i/\Gamma_{rad}))$. The ratio $\Gamma_i/\Gamma_{rad}$ for a smooth thin metal film on a dielectric substrate can be calculated analytically starting from the complex SP wavevector $k_x = k_x' + ik_x''$ of a two-layer semi-infinite cover–metal in-

terface. One can obtain an expression for the complex change in the SP wavevector ($\Delta k_x$) when the metal thickness is reduced in the presence of a dielectric substrate [5];

$$\Delta k_x = r_{sm}^{TM} \cdot e^{-2ik''_{z,m}d} \cdot 2\frac{\omega}{c}\left(\frac{\varepsilon_m \varepsilon_c}{\varepsilon_m + \varepsilon_c}\right)^{3/2} \cdot \left(\frac{1}{\varepsilon_c - \varepsilon_m}\right) \quad (1)$$

where $\varepsilon_m$ and $\varepsilon_c$ are the complex dielectric constants of the metal film and the cover layer respectively, and $r_{sm}^{TM}$ is the electric field amplitude reflection coefficient of the substrate–metal interface for TM-polarized light incident on the metal from the substrate side. Since $k_x''$ is proportional to $\Gamma_i$, and $\Delta k_x''$ is proportional to the added radiative damping $\Gamma_{rad}$, we have $\Gamma_i/\Gamma_{rad} \approx k_x''/\Delta k_x''$. Based on the thus obtained values for $\Gamma_i/\Gamma_{rad}$ we can now determine the frequency dependent coupling efficiency $\eta_{SP}$ by measuring $P_{SP,rad}$ and $P_{inc}$. The frequency-dependent SP excitation efficiency can therefore be obtained through a simple comparison of the measured radiated and transmitted power, combined with an either calculated or measured transmissivity and the analytically calculated SP wavevectors.

**3 Experimental** A 5 nm Cr adhesion layer was deposited onto the glass substrate, followed by thermal evaporation of a 55 nm Au layer and plasma-enhanced chemical vapor deposition of a 30 nm $SiO_2$ spacer layer. Nanoparticle arrays were fabricated on the $SiO_2$ spacer layer using standard electron-beam lithography techniques. The nanoparticles were designed to be 35 nm thick, 130 nm long in the $x$-direction, and 50 nm wide in the $y$-direction, resulting in an in-plane aspect ratio (AR = length/width) of 2.6. A 5 nm Cr wetting layer was used to promote adhesion to the $SiO_2$ spacer layer. The particles had a constant center-to-center spacing in the $x$- and $y$-directions of 600 nm and 280 nm respectively. The array contains 20 and 54 periods in the $x$- and $y$-direction respectively, giving an array size of approximately 10 μm × 15 μm.

A sketch of the measurement setup is shown in Fig. 1. The sample was top-illuminated using a standard halogen light source, via a condenser of numerical aperture (N.A.) 0.15. The incident light was polarized along the $x$-direction before entering the condenser, leading to grating mediated

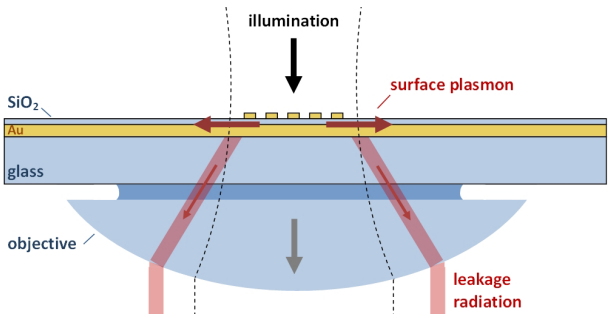


**Figure 1** (online colour at: www.pss-rapid.com) Schematic of the experimental setup, showing the collection of leakage radiation using an oil immersion objective.

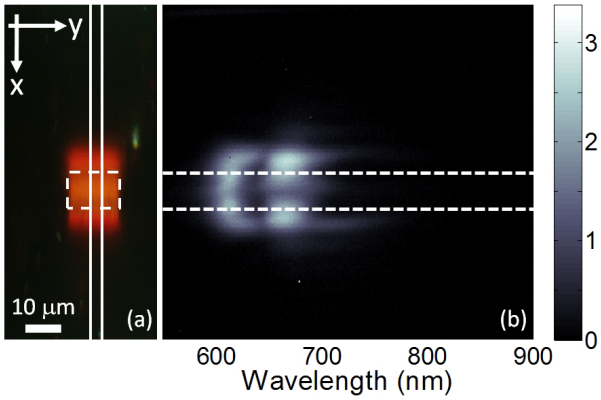


**Figure 2** (online color at: www.pss-rapid.com) (a) Leakage radiation image of SPs excited by the array. (b) Spectral image of the leakage radiation collected from the area between the vertical solid lines in (a). The horizontal dashed lines mark the location of the edges of the array.

excitation of SPs propagating in the $x$-direction. The generated LR was collected with a 60× oil immersion objective with a N.A. of 1.25 using index matching oil ($n$ = 1.516) between the substrate and the objective (dark blue region in Fig. 1). The zero order transmission (gray arrow in Fig. 1) was blocked, allowing the selective imaging of LR generated by propagating SPs. For spectral analysis the collected LR was projected onto the entrance slit of an imaging spectrometer (Horiba Jobin Yvon iHR-320). Spectra were recorded using a Si charge coupled device and corrected for the detector dark current. The entrance slit width was set to 50 μm, resulting in a spectral resolution of 7 nm.

**4 Results and discussion** Figure 2a shows an image of the collected LR, recorded using a digital camera. The dashed rectangle marks the location of the array. SPs can be seen propagating in the positive and negative $x$-directions. The image collection region for spectral analysis is shown schematically by the solid lines in Fig. 2a. Figure 2b shows the obtained spatially resolved LR spectrum. The vertical direction in the image corresponds to the position along the direction of SP propagation ($x$-direction) on the same scale as Fig. 2a. The color represents the intensity of the LR at each wavelength and spatial coordinate. The dashed horizontal lines mark the edges of the array.

The radiated LR signal $S_{LR}$ was measured by spatially integrating the signal corresponding to SPs propagating away from the array, corresponding to the regions above and below the dashed lines in Fig. 2b. The transmitted signal $S_T$ through an unpatterned region of the deposited Au film was collected over an area equal to the array size (area between the solid and dashed lines in Fig. 2a) using the same detection parameters as used for $S_{LR}$. Figure 3a shows the resulting ratio $S_{LR}/S_T$. Since both $S_{LR}$ and $S_T$ contain the illumination spectrum and the wavelength dependent detector sensitivity, we obtain $S_{LR}/S_T = P_{SP,rad}/P_T$ with $P_T$ the transmitted power through an Au coated area equivalent to the array size.

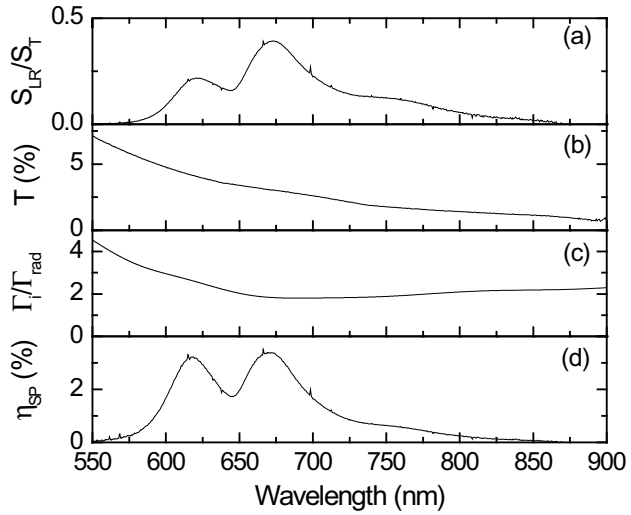


**Figure 3** (a) Leakage radiation spectrum normalized to the film transmission, (b) transmissivity of the Au film, (c) calculated ratio $\Gamma_i/\Gamma_{rad}$, and (d) wavelength dependent SP coupling efficiency.

Figure 3b shows the obtained transmissivity of the unpatterned film given by $T = (1 - R_s)\, S_T/S_s$, where $R_s = 0.04$ is the reflectivity of the uncoated glass substrate and $S_s$ is the transmitted signal through the substrate measured in an uncoated and unpatterned region of the sample. Figure 3c shows the wavelength dependent ratio $\Gamma_i/\Gamma_{rad}$ calculated based on Eq. (1) in combination with literature values for the material properties [6] and the known layer thicknesses. Note that scattering of SPs by film roughness was neglected in this analysis. To account for the 30 nm $SiO_2$ spacer layer, an effective dielectric function $\varepsilon_c = 1.05$ was used for the cover layer in the calculations of $\Delta k_x$. The bottom 5 nm Cr adhesion layer was replaced in the calculation by an additional 5 nm of Au.

Figure 3d shows the obtained spectral coupling efficiency $\eta_{SP}$ of the nanoparticle grating coupler using the values of $P_{SP,rad}/P_T$, $T$, $\Gamma_i/\Gamma_{rad}$, and using $P_T = P_{inc} \times T$. Two main peaks are observed in the efficiency of SP excitation. Based on the grating spacing and the SP dispersion, it is expected that under normal plane-wave illumination SPs excited by each row of particles will interfere constructively with the SPs excited by neighboring rows for a free-space wavelength of approximately 630 nm. The two main peaks in the efficiency lie above and below the expected wavelength of the grating resonance. A previous study [7] of NP arrays near a thick metal film has shown that these two peaks correspond to grating modes excited by the $x$- and $z$-polarization components of the illumination, and are a consequence of convergent illumination. N.A. dependent measurements (not shown) suggest that the peak near 670 nm corresponds to the $z$-polarized grating mode, and the peak near 615 nm corresponds to the $x$-polarized grating mode. In addition to the two grating related SP excitation peaks, a broad and weak peak is observed at approximately 770 nm. Excitation of SPs at wavelengths this far from grating resonance seems counter-intuitive, since no constructive addition of SP amplitude is possible. However, individual Au nanoparticles support a dipolar plasmon resonance, which for isolated ellipsoidal Au nanoparticles of this aspect ratio is predicted to occur at 592 nm in air, and at 727 nm in $SiO_2$ based on literature dielectric functions. The relatively large size of the particles will lead to a red-shift of the resonance, and interaction with the metal surface will lead to an additional red-shift due to the excitation of an oscillatory image charge distribution [8]. We therefore attribute the peak at 770 nm to the particle resonance enhanced excitation of SPs by the rows of particles near the edge of the array.

The maximum efficiency of the structure of ~3.5% observed in Fig. 3d occurs at the two grating resonances. Note that this figure indicates the useful excited SP power, i.e. it does not include any SP power dissipated within the excitation structure. This efficiency represents a lower limit on the achievable coupling efficiency since the illumination N.A. was not optimized for this specific structure.

**5 Conclusion** The wavelength dependent surface plasmon excitation efficiency of a miniature nanoparticle enhanced grating coupler was determined using spatially resolved leakage radiation spectroscopy. A broadly applicable method for determining the wavelength dependent efficiency of a plasmon coupler exciting propagating SPs on a thin metal film was developed. The maximum observed surface plasmon coupling efficiency was 3.5%.

**Acknowledgements** This work was supported by the National Science Foundation (CAREER Award No. ECCS-0644228).

## References

[1] B. Steinberger, A. Hohenau, H. Ditlbacher, A. L. Stepanov, A. Drezet, F. R. Aussenegg, A. Leitner, and J. R. Krenn, Appl. Phys. Lett. **88**, 094104 (2006).
[2] J.-C. Weeber, Y. Lacroute, and A. Dereux, Phys. Rev. B **68**, 115401 (2003).
[3] D. F. P. Pile, D. K. Gramotnev, M. Haraguchi, T. Okamoto, and M. Fukui, J. Appl. Phys. **100**, 013101 (2006).
[4] K. Tanaka, M. Tanaka, and T. Sugiyama, Opt. Express **13**, 256 (2005).
[5] H. Raether, Surface Plasmons on Smooth and Rough Surfaces and on Gratings (Springer-Verlag, Berlin, 1988).
[6] P. B. Johnson and R. W. Christy, Phys. Rev. B **6**, 4370 (1972).
[7] A. Ghoshal, I. Divliansky, and P. G. Kik, Appl. Phys. Lett. **94**, 171108 (2009).
[8] Min Hu, Amitabh Ghoshal, M. Marquez, and P. G. Kik, J. Phys. Chem. C **144**, 7509 (2010).